Energy Dispersion of $4f$-Derived Emissions in Photoelectron Spectra of the Heavy-Fermion Compound $YbIr_2Si_2$

S. Danzenbächer,[1] Yu. Kucherenko,[1,2] C. Laubschat,[1] D. V. Vyalikh,[1] Z. Hossain,[3,4] C. Geibel,[3] X. J. Zhou,[5,6] W. L. Yang,[5,6] N. Mannella,[5,6] Z. Hussain,[6] Z.-X. Shen,[5] and S. L. Molodtsov[1]

[1]*Institut für Festkörperphysik, Technische Universität Dresden, D-01062 Dresden, Germany*
[2]*Institute of Metal Physics, National Academy of Sciences of Ukraine, UA-03142 Kiev, Ukraine*
[3]*Max-Planck-Institut für Chemische Physik fester Stoffe, Nöthnitzer Strasse 40, D-01187 Dresden, Germany*
[4]*Department of Physics, Indian Institute of Technology, Kanpur-208016, India*
[5]*Department of Physics, Applied Physics and Stanford Synchrotron Radiation Laboratory, Stanford University, Stanford, California 94305, USA*
[6]*Advanced Light Source, Lawrence Berkeley National Laboratory, Berkeley, California 94720, USA*

(Received 15 July 2005; published 17 March 2006)

Angle-resolved photoemission spectra of the heavy-fermion system $YbIr_2Si_2$ are reported that reveal strong momentum ($\mathbf{k}$) dependent splittings of the $4f^{13}$ bulk and surface emissions around the expected intersection points of the $4f$ final states with valence bands in the Brillouin zone. The obtained dispersion is explained in terms of a simplified periodic Anderson model by a $\mathbf{k}$ dependence of the electron hopping matrix element disregarding clearly interpretation in terms of a single-impurity model.

DOI: 10.1103/PhysRevLett.96.106402 PACS numbers: 71.27.+a, 71.20.Eh, 75.30.Mb, 79.60.−i

Heavy-fermion (HF) systems are characterized by quasiparticle bands of large effective masses close to the Fermi energy (E_F) that govern the thermodynamic, transport and in part magnetic properties of these materials [1–4]. In the case of rare-earth compounds, the quasiparticle states arise from many-body interactions of valence states with the strongly localized $4f$ states. Here, particularly the single-impurity Anderson model (SIAM) has successfully been applied in many cases for the description of HF properties [5]. Nevertheless, the question as to whether it is sufficient to treat the f states as localized impurities or the crystal symmetry has to be considered like in the periodic Anderson model (PAM) [6] remains a subject of extensive debates until now.

A possible momentum ($\mathbf{k}$) dependence of hybridization may have severe consequences on the material properties [7]. Unfortunately, a satisfactory solution of PAM that takes into account a realistic band structure of non-f derived states is still missing. Most direct experimental insight into this problem may be expected from angle-resolved photoemission (PE) experiments that reflect the momentum resolved response of the electronic system to a single $4f$ excitation, while transport, specific heat, and magnetization measurements integrate over many different excitations and large areas in $\mathbf{k}$ space. Yb compounds are well suited for exactly this purpose, since due to the almost occupied Yb $4f$ shell the Kondo resonance is found below the Fermi energy and fully accessible to PE experiments.

High-resolution PE experiments on single-crystalline samples of HF systems like $YbAl_3$ [8,9], $YbCu_2Si_2$ [8,10], YbB_{12} [11], and $YbInCu_4$ [12] were reported. However, controversial conclusions were derived about the applicability of the SIAM to the description of position, shape, and temperature dependence of the Kondo resonance. A possible $\mathbf{k}$ dependence of the $4f$ emission has not been observed so far for Yb systems. For Ce systems, intensity changes of the Kondo peak were reported in a few cases that were attributed to a $\mathbf{k}$ dependent variation of the hybridization [13]. Dispersion, however, if present at all, was found to be not larger than 30 meV [14].

In the present Letter we report the first observation of strong dispersions and energy splittings of the $4f$ states in the HF compound $YbIr_2Si_2$. These effects, which are not only restricted to the vicinity of the Fermi energy, but also observed for the surface $4f$ emission at higher binding energy (BE), clearly ruled out an interpretation in terms of the SIAM. Instead, we show that the data may correctly be described within a simple approach to the PAM.

Single-crystalline $YbIr_2Si_2$ samples [body-centered tetragonal $ThCr_2Si_2$- (I-) type [15]] were grown from In flux in a closed Ta crucible and characterized by x-ray diffraction as well as by magnetic susceptibility, resistivity, and specific heat measurements [16]. The measured Kondo temperature $T_K \sim 40$ K is almost twice the value reported for $YbRh_2Si_2$ [17]. Both compounds are close to a quantum critical point, where magnetic ordering via RKKY interactions is balanced by Kondo screening. In contrast to the Rh compound, no magnetic ordering below T_K was observed in $YbIr_2Si_2$.

Angle-resolved PE experiments were performed at beam line 10.0.1 (Advanced Light Source) using the experimental station HERS equipped with a Scienta R4000 analyzer. The samples were cleaved *in situ* in a vacuum with a base pressure better than 5×10^{-11} Torr, and measured in the Kondo regime at a temperature of ~20 K. The beam polarization was in the sample plane perpendicular to the $\bar{\Gamma}$-$\bar{M}$ direction, with the beam nearly at grazing incidence with the sample surface. The spectra were acquired in the angle mode, where 30° cuts parallel to the $\bar{\Gamma}$-$\bar{M}$ were

covered. Angular and energy resolutions were set to 0.3° and 20 meV, respectively.

Figure 1 shows angle-integrated PE spectra taken at two different photon energies: At $h\nu = 25$ eV the $4f$ cross section is almost zero and the spectrum is dominated by emissions from the Ir $5d$-derived bands, that are centered around 2.2 eV BE and reveal a width of about 2 eV. At $h\nu = 110$ eV, on the other hand, the cross section of the Yb $4f$ states is large, while the contributions from the valence bands are negligible. Between 5 and 13 eV BE, PE lines of a Yb $4f^{12}$ final-state multiplet are observed, while two $4f^{13}$ doublets appear close to E_F and at 0.9 eV corresponding to signals from bulk and surface, respectively. BE and intensity of the surface emission vary from sample to sample reflecting the actual termination of the sample surface that ranges from a closed Yb layer to a Si layer with few Yb adatoms. From the coexistence of the $4f^{12}$ and $4f^{13}$ bulk emissions a mixed-valent ground state can be concluded. The spectra were least-squares fitted by a superposition of $4f^{12}$ and $4f^{13}$ multiplets [18] and a weak integral background. Best fits were obtained with nearly symmetric Doniach-Sunjič line shapes convoluted by a Gaussian (20 meV FWHM) to account for the finite energy resolution. From the intensity ratio of the $4f^{13}$ and $4f^{12}$ bulk emissions a mean valence of 2.9 is derived.

Figure 2 presents a series of angle-resolved PE spectra acquired along the $\bar{\Gamma}$-$\bar{M}$ direction at different detection angles, Θ. A photon energy of 55 eV was chosen in order to make not only $4f$ but also VB emissions visible. Two parabolic VBs with a holelike dispersion are observed, from which one intersects the $4f_{7/2}$ surface emission close to $\bar{\Gamma}$. Around the intersection point, the $4f$ surface signal at 0.6 eV BE splits into at least two dispersive components separated from each other by up to 0.25 eV. In the same $\mathbf{k}$ region three further peaks are observed at 0.30, 0.15, and 0.05 eV. The 0.05-eV feature represents the Kondo resonance. The 0.15-eV feature appears as a shoulder in the 110-eV data and might, therefore, originate from a $4f$ emission, while the 0.30-eV structure is not seen in Fig. 1 and reflects probably a VB emission.

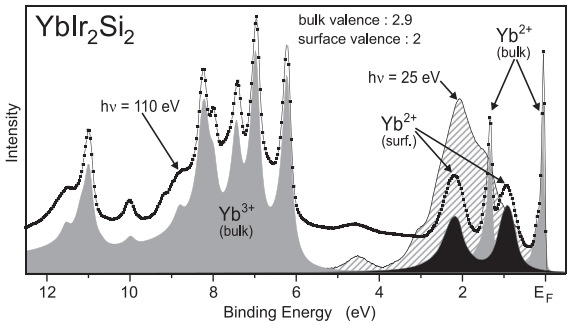

FIG. 1. PE spectra of $YbIr_2Si_2$ taken at 25 (hatched) and 110 eV (dots) photon energy integrated in the range of angles from $-5°$ to $+25°$ to the normal emission along the $\bar{\Gamma}$-$\bar{M}$ direction. Subspectra reflect results of a least-squares fit using atomic Yb $4f^{12}$ and $4f^{13}$ final-state multiplets [18].

Figure 3 (left) shows results of band-structure calculations performed for $YbIr_2Si_2$ by means of a fully relativistic version [19] of the linear muffin-tin orbitals (LMTO) method [20]. Surface effects were accounted for by consideration of a nine-atomic layer slab with (001) orientation of the surface. The $4f$ states appear as narrow spin-orbit-split bands close to E_F and at $\sim$1.5 eV BE. For the surface layer almost the same BE position of the $4f$ band is obtained as for the bulk, in contrast to the experimental observation. This clearly illustrates that local density approximation does not describe correctly the many-body properties of the f states.

In order to extract the structure of the VBs without the $4f$ states, Yb atoms were replaced in the calculations by trivalent La in the bulk and by divalent Ba at the surface (Fig. 3, right). Around Γ a group of parabolic bands with holelike dispersions is observed between 0.5 and 1.5 eV BE. Another group of VBs with electronlike dispersions is found close to E_F. Apart from a small shift of about 0.1 eV to higher BE, these theoretical results are in good agreement with our experimental data.

The starting point of our theoretical analysis of the $4f$ emission in $YbIr_2Si_2$ was a simplified PAM [13]. Parameters of the model are the energy of the unhybridized f state $\varepsilon_f(\mathbf{k}) = \varepsilon_f$, the hybridization $V_{\mathbf{k}}(\varepsilon)$ and the on-site Coulomb repulsion U_{ff}. In the present analysis f holes (h) instead of f electrons were considered, taking into account the nearly filled $4f$ shell of Yb. After some algebra and redefining of model parameters, one gets as basis states the h^0 ($4f^{14}$), energy of which is set to zero, the h^1 ($4f^{13}$) corresponding to energy ε_f, and the h^2 ($4f^{12}$) configuration with energy $2\varepsilon_f + U_{ff}$, in analogy to the notation applied for electron states in Ce compounds.

The main difficulty in treating the PAM relates to the local Coulomb interaction, U_{ff}. Transformation of this

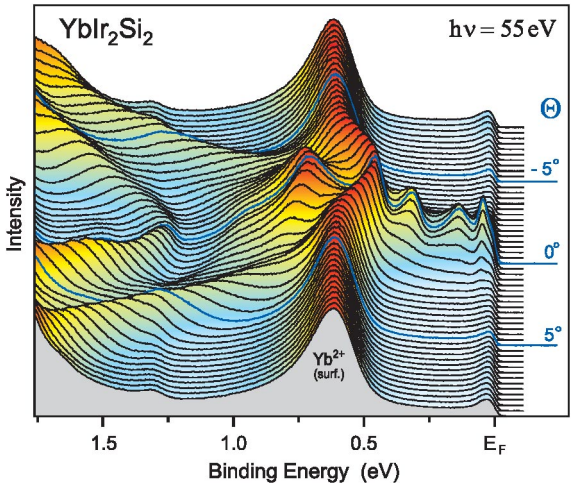

FIG. 2 (color). Angle-resolved PE spectra of $YbIr_2Si_2$ taken along the $\bar{\Gamma}$-$\bar{M}$ direction. Note that the surface-to-bulk ratio of the $4f$ signal is larger and the BE of the $4f$ surface component is smaller than that in the $4f$ spectrum shown in Fig. 1, indicating surface termination by an almost closed Yb layer [23].

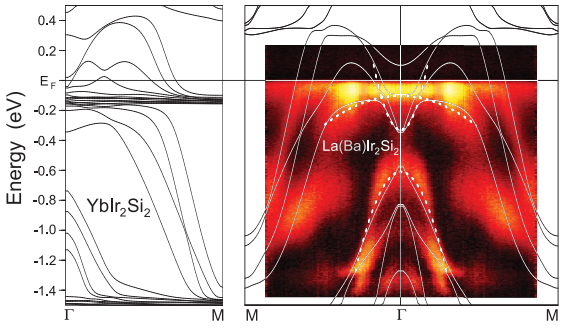

FIG. 3 (color). Energy bands calculated along the Γ-M direction of the Brillouin zone for the nine-atomic layer $YbIr_2Si_2$ slab (left) and for the slab, where Yb atoms are substituted by Ba in the surface layer and by La in the bulk (right). For comparison, experimental PE data taken at $h\nu = 25$ eV are shown in a color-scale representation, where lighter colors correspond to higher PE intensities.

term to a $\mathbf{k}$ representation leads to a mixing of states with different $\mathbf{k}$ values that makes the problem complex to handle quantitatively. Neglecting weak contributions of the h^2 ($4f^{12}$) configurations to the initial- and final-state configurations ($U_{ff} \rightarrow \infty$) results in $\mathbf{k}$ conservation and allows the diagonalization of the Hamiltonian for each particular $\mathbf{k}$ point of the Brillouin zone (BZ).

In contrast to Ce, however, the h^2 configuration may be neglected only for the divalent surface atoms, while for the mixed-valent bulk atoms the h^2 term is essential for description of the $4f^{12}$ PE final state. Nonetheless, since the energy separation between the h^2 ($4f^{12}$) and the energetically nearly degenerated h^1 ($4f^{13}$) and h^0 ($4f^{14}$) configurations is large, h^2 admixtures to the ground and PE final states close to E_F, are expected to be weak.

As a first step of our treatment we used the calculated VB structure of $La(Ba)Ir_2Si_2$ (see Fig. 3, right). Since, due to symmetry requirements, a coupling of the $4f$ states is only expected to VB states with non-negligible local f character at the Yb sites, we calculated the respective f-projected local expansion coefficients $c_f(E, \mathbf{k})$ of the Bloch functions around the Yb sites and wrote for the $\mathbf{k}$ dependent hybridization matrix element

$$V_{\mathbf{k}}(E) = \Delta c_f(E, \mathbf{k}), \tag{1}$$

where Δ (like ε_f) is a constant, adjustable parameter. The second step was the calculation of the spectral function on the basis of the simplified PAM assuming $\mathbf{k}$ conservation. In the region of interest close to the Γ point we approximated three main bands by parabolic functions as shown by dots in the right panel of Fig. 3 and as insets in Fig. 4 with $c_f(E, \mathbf{k})$ values similar to those for the original bands. Spectral functions were calculated for the individual layers of the slab and finally superimposed on each other in order to simulate the PE spectra. To this end, contributions of the Yb surface and bulk (fifth bulk layer in the slab) layers were weighted by a factor of 0.71 and 0.29, respectively, in order to account for an exponential dependence of the escape depth of the $4f$ photoelectrons.

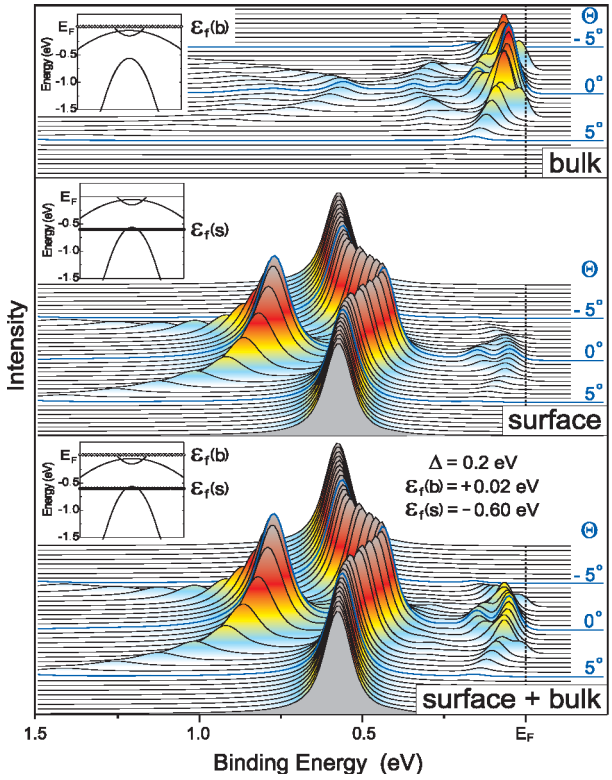

FIG. 4 (color). Angle-resolved $4f$ emission of $YbIr_2Si_2$ simulated by means of the simplified PAM: contribution from the bulk (top, multiplied by factor 3.5), the surface layer (middle), and the total intensity distribution in the PE spectra (bottom).

The numerical treatment is similar to that of the SIAM [21]. The fundamental difference, however, is that instead of a density of states integrated over the whole BZ, a $\mathbf{k}$ dependent energy distribution of VB states is used. A series of calculated spectral functions along the Γ-M direction is shown in Fig. 4. The spectral functions were obtained using the parameters $\varepsilon_f(b) = 0.02$ eV and $\Delta = 0.2$ eV [for the surface, ε_f was lowered to $\varepsilon_f(s) = -0.6$ eV]. A choice of $\varepsilon_f(b)$ immediately above E_F was necessary, because the system is mixed valent with a mean valency close to 3. An estimate of $\varepsilon_f(s)$ is obtained from the observed BE of the unhybridized $4f_{7/2}$ surface signal and Δ is determined from the hybridization-induced splitting of the $4f$ surface signal. The actual parameters were then derived from the best fit to the experimental data. Taking into account the increase of the recombination rate of the photoholes with BE, an energy dependent lifetime broadening of the form $\Gamma_L = 0.01$ eV $+ 0.08E$ was used, where E denotes the BE with respect to E_F [21]. The calculated spectral functions were additionally broadened with a Gaussian ($\Gamma_G = 20$ meV) to simulate the finite instrumental resolution.

Beginning with the discussion of the surface component, the calculated spectra shown in the middle of Fig. 4 reproduce nicely the observed dispersion of the $4f$ states around the $\bar{\Gamma}$ point. The large splitting of the main surface

emission around 0.6 eV BE is due to the formation of symmetric and antisymmetric linear combinations of the $4f$ and VB orbitals lifting the energy degeneracy of these states. In addition to the splitting of the main $4f$ surface component, further f-derived surface features appear at lower BE. These structures reflect a similar phenomenon as the Abrikosov-Suhl resonance observed in PE spectra of Ce systems [21,22] and arise from f admixtures to valence bands laying at lower binding energies.

In the case of the bulk emission, no f contributions around E_F are expected without hybridization at $T = 0$ K, because the divalent $4f^{14}$ configuration lies above the Fermi energy and is unoccupied. For finite hybridization and a VB state around 0.05 eV BE, however, two peaks appear in the simulated PE spectra at about 0.05 eV and 0.15 eV BE in agreement with the experiment (Fig. 4, upper panel). These peaks reflect symmetric and antisymmetric linear combinations of $4f^{13}$ and $4f^{14}$ configurations. Deeper lying VB states cause additional features at correspondingly higher BEs, the intensities of which decrease with increasing binding energy. The lowest lying f-derived feature appears at the BE of the lowest occupied VB and reveals the same dispersion as the latter with the consequence that the feature disappears at the crossing of the Fermi energy by the VB state.

Superposition of the bulk and surface contributions in the bottom of Fig. 4 yields impressive agreement with the experimental data. One may notice, however, that even far from the $\bar{\Gamma}$ point finite spectral weight at E_F is observed in the experimental data that is not reproduced by our numerical approach. This feature may be assigned to thermal excitation into the bulk $4f$ state closely above E_F [22]. On the other hand, effects of finite U_{ff} and interaction of the $4f$ with unoccupied VB states, which were not considered in the present model, may also contribute to this peak.

In summary, we have found that the $4f$ states in $YbIr_2Si_2$ are subject to strong **k** dependent splittings and dispersions, a behavior which cannot be understood in the framework of SIAM. We could show that the $4f$ PE data are correctly described within a simple approach to PAM in the limit $U_{ff} \rightarrow \infty$. In this approach, energy splittings and dispersion of the $4f$ states are predicted for those points in **k** space where VB states are degenerate in energy with unhybridized $4f^n$ configurations. Since for mixed-valent systems this condition is particularly fulfilled at the Fermi surface, our results may have strong impact on the understanding of the HF properties. The dispersive properties of the $4f$ states explain in a natural way the observed broadening and line shape anomalies in angle-integrated PE spectra of many Yb systems as well as discrepancies between the angle-resolved PE data of different authors.

This research was funded by the Deutsche Forschungsgemeinschaft, SFB 463, Projects TP B4 and TP B16, the BMBF, Project No. 05-SF8OD1/4. The experiments at the ALS and SSRL were supported by the DOE's Office of BES, Division of Material Science, with Contract No. DE-FG03-01ER45929-A001. The work at Stanford was also supported by NSF Grant No. DMR-0304981 and ONR Grant No. N00014-98-1-0195-P0007.

[1] P. Fulde, *Electron Correlations in Molecules and Solid* (Springer, Heidelberg, 1995).
[2] P. Wachter, *Intermediate Valence and Heavy Fermions*, edited by K. A. Gschneider, L. Eyring, G. H. Lander, and G. R. Choppin, Handbook on the Physics and Chemistry of Rare Earth Vol. 19 (Elsevier Science, New York, 1994).
[3] L. Degiorgi, Rev. Mod. Phys. **71**, 687 (1999).
[4] A. C. Hewson, *The Kondo Problem to Heavy Fermions* (Cambridge University Press, Cambridge, England, 1993).
[5] P. W. Anderson, Phys. Rev. **124**, 41 (1961); O. Gunnarsson and K. Schönhammer, Phys. Rev. Lett. **50**, 604 (1983); Phys. Rev. B **28**, 4315 (1983).
[6] A. N. Tahvildar-Zadeh *et al.*, Phys. Rev. Lett. **80**, 5168 (1998); M.-W. Xiao *et al.*, Phys. Rev. B **65**, 235122 (2002).
[7] S. Doniach, Phys. Rev. B **35**, 1814 (1987).
[8] J. J. Joyce *et al.*, Phys. Rev. B **54**, 17 515 (1996); R. I. R. Blyth *et al.*, Phys. Rev. B **48**, 9497 (1993).
[9] J. J. Joyce *et al.*, Phys. Rev. Lett. **72**, 1774 (1994).
[10] J. M. Lawrence *et al.*, J. Magn. Magn. Mater. **108**, 215 (1992).
[11] T. Susaki *et al.*, Phys. Rev. Lett. **82**, 992 (1999); J. J. Joyce and A. J. Arko, Phys. Rev. Lett. **78**, 1831 (1997); T. Susaki *et al.*, Phys. Rev. B **56**, 13 727 (1997); T. Susaki *et al.*, Phys. Rev. Lett. **77**, 4269 (1996).
[12] K. Yoshikawa *et al.*, Phys. Rev. B **72**, 165106 (2005); H. Sato *et al.*, Phys. Rev. Lett. **93**, 246404 (2004); H. Sato *et al.*, Phys. Rev. B **69**, 165101 (2004); F. Reinert *et al.*, Phys. Rev. B **63**, 197102 (2001); J. J. Joyce *et al.*, Phys. Rev. B **63**, 197101 (2001); D. P. Moore *et al.*, Phys. Rev. B **62**, 16 492 (2000); F. Reinert *et al.*, Phys. Rev. B **58**, 12 808 (1998).
[13] S. Danzenbächer *et al.*, Phys. Rev. B **72**, 033104 (2005).
[14] A. B. Andrews *et al.*, Phys. Rev. B **53**, 3317 (1996); H. Kumigashira *et al.*, Phys. Rev. B **54**, 9341 (1996); **55**, R3355 (1997); A. J. Arko *et al.*, Phys. Rev. B **56**, R7041 (1997); M. Garnier *et al.*, Phys. Rev. B **56**, R11 399 (1997); J. Boysen *et al.*, J. Alloys Compd. **275–277**, 493 (1998).
[15] H. F. Braun *et al.*, Phys. Rev. B **28**, 1389 (1983).
[16] Z. Hossain *et al.*, Phys. Rev. B **72**, 094411 (2005).
[17] O. Trovarelli *et al.*, Phys. Rev. Lett. **85**, 626 (2000); P. Gegenwart *et al.*, Phys. Rev. Lett. **89**, 056402 (2002); J. Custers *et al.*, Nature (London) **424**, 524 (2003); J. Sichelschmidt *et al.*, Phys. Rev. Lett. **91**, 156401 (2003).
[18] F. Gerken, J. Phys. F **13**, 703 (1983).
[19] V. V. Nemoshkalenko *et al.*, Phys. Status Solidi B **120**, 283 (1983).
[20] O. K. Andersen, Phys. Rev. B **12**, 3060 (1975).
[21] R. Hayn *et al.*, Phys. Rev. B **64**, 115106 (2001).
[22] F. Reinert *et al.*, Phys. Rev. Lett. **87**, 106401 (2001).
[23] W. D. Schneider *et al.*, Phys. Rev. B **27**, 6538 (1983).